nzsee
NEW ZEALAND SOCIETY FOR EARTHQUAKE ENGINEERING

# Towards a better understanding of the development of the strength in Asymmetric Friction Connections

*J.C. Chanchi Golondrino*
Universidad Nacional de Colombia, Departamento de Ingeniería Civil, Manizales, Colombia.

*G.A. MacRae*
University of Canterbury, Department of Civil and Natural Resources, Christchurch.

*J.G. Chase & G.W. Rodgers*
University of Canterbury, Department of Mechanical Engineering, Christchurch.

*G.C. Clifton*
The University of Auckland, Department of Civil & Environmental Engineering, Auckland.

## ABSTRACT

In the current design practice, the strength of Asymmetric Friction Connections (AFCs) is calculated considering the friction force developed at both sliding interfaces using the bolt tension reduced by the moment – shear - axial interaction (MPV) effect. However, available models do not consider the friction induced by the bolt assembly force, termed assembly effect, or the bolt inclination effect, which is the increase in the AFC strength due to the horizontal component of the bolt tension produced when the bolt inclines. This paper proposes a model for quantifying the strength of AFCs considering the assembly, MPV, and inclination effects for the cases: i). Before the slotted plate breakaway, ii). Bolts inclining up to the angle defined by the bole hole oversize and termed bolt elastic inclination, iii) Bolts inclination angles larger than the angle defined by the bole hole oversize and produced by bolt flexural yielding and termed bolt yielding inclination. The proposed model is validated from the testing of an AFC scaled prototype, and from the quasi – static testing of 18 AFCs in real scale and assembled with Bisalloy 500 shims, and 2 M16 Grade 8.8 bolts with bolt grip lengths between 52.5mm and 172.5mm. It is shown that before breakaway the hysteresis loop is linear, and the peak strength depends only on the assembly effect. For the bolt elastic inclination, the hysteresis loop shape is bilinear, and the peak strength depends on the combined action of the assembly, MPV, and inclination effects. For the bolt yielding inclination, the hysteresis loop is square and pinched and the average strength across the plateau of the hysteresis loop depends on the MPV and inclination effects. For the three cases considered, the

proposed model predicts the AFC strength with accuracies of 76% – 120%. The proposed model shows the horizontal component of the bolt tension from the bolt inclination effect was 6% - 28% of the AFC strength for the bolt elastic inclination, and 38% - 53% of the AFC strength for the bolt yielding inclination.

## 1 INTRODUCTION

Asymmetric Friction Connections (AFCs) are bolted friction connections used to dissipate seismic energy (Clifton 2005). AFCs are assembled with a slotted plate, two thin plates termed shims, and two external plates, one plate with restricted displacement and termed fixed plate, and the other plate is a floating plate termed cap plate, as shown in Figure 1a. The slotted, fixed and cap plates are made of Grade 300 steel, and the shims are made of a high hardness material such as Bisalloy 500 shims (Bisalloy Steels Pty Ltd, 2006). These set of plates are clamped together by means of high strength bolts such Grade 8.8 bolts. In AFCs energy is dissipated when the slotted plate is pushed axially until overcoming the friction force induced by the high strength bolts on the top shim – slotted plate and bottom shim – slotted plate interfaces producing an almost rectangular hysteresis loop (Rodgers et al. 2017). The average force across the plateau of the hysteresis loop is termed sliding strength, and is almost constant for AFCs assembled with Grade 300 steel plates and Bisalloy 500 shims (Chanchi et al. 2019a). AFCs can be used as seismic dissipaters in beam column joints (Clifton 2005, MacRae et al. 2010), within braces (Xie et al. 2018), and in column bases (Borzouie et al. 2015).

The sliding strength have been observed to reduce as the bolt grip length is increased (Clifton 2005). This reduction in sliding strength was attributed to the reduction in bolt tension occurring when the bolt inclines and bears on the cap plate and fixed plate, generating simultaneously moment, shear, and axial demands on the bolt shank, as shown in Figures 1 (Clifton 2005). This bolt behaviour is termed moment – axial – shear interaction (MPV), and is based on the reduction in axial tension when the bolt moment demand increases as the distance between the bolt bearing points termed bolt lever arm, $l$, increases (Khoo et al. 2014).

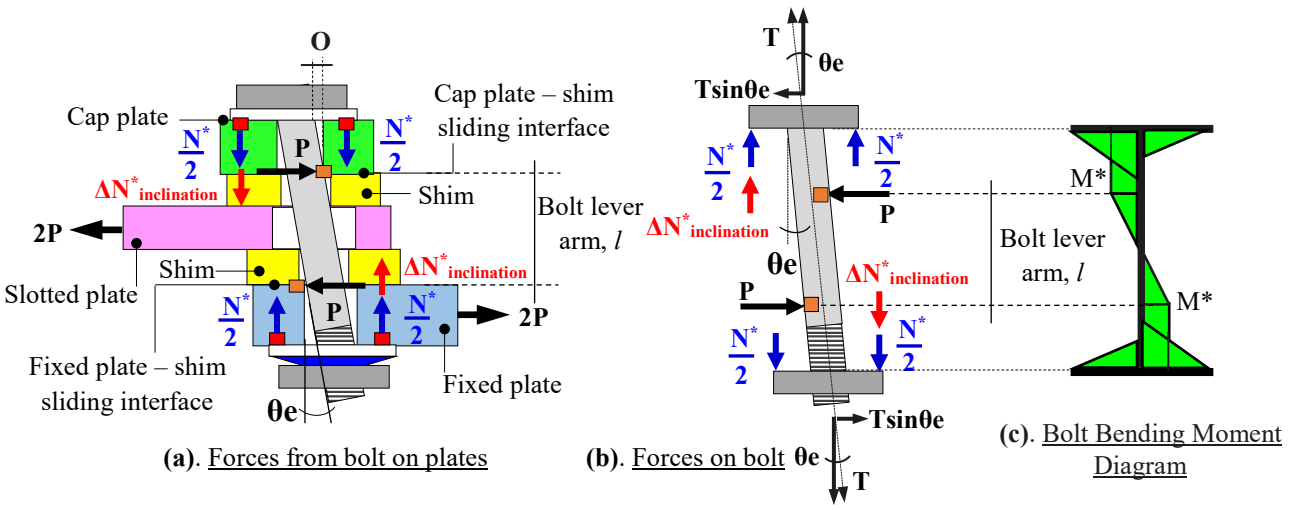


*Figure 1: Idealized model of bolt under MPV in AFCs (Clifton 2005, Khoo et al. 2014, Chanchi Golondrino et al. 2019)*

Models for quantifying the bolt tension during the sliding, $T$, which is the assembly bolt tension, $N^*$, minus the reduction in bolt tension due to MPV effect, were proposed by Clifton 2005 and Khoo et al. 2014. These MPV models were based on considering the bolt vertical during the sliding of the slotted plate, and they ignore the increase in bolt tension due to bolt inclination, $\Delta N^*_{inclination}$, shown in Figure 1b. Clifton 2005 and

Khoo et al. 2014 MPV models use the following interaction equation to represent the combined action of the moment, axial, and shear on the bolt:

$$\left[\frac{M^*}{M_{rfn}}\right]+\left[\frac{V^*}{V_{rfn}}\right]=1 \quad (1)$$

Where, $M^*$ is the bolt moment demand, $V^*$ is the bolt shear demand, $M_{rfn}$ is the nominal bolt moment capacity considering axial force interaction using the bolt tension during the sliding, $T$, $V_{rfn}$ is the nominal bolt shear capacity considering no axial force interaction. These variables are defined:

$$V^* = T \times \mu \quad (2)$$

$$M^* = \frac{T \times \mu \times l}{2} \quad (3)$$

$$M_{rfn} = 0.1665 \times d^3 \times \left[1-\left[\frac{T}{0.56 \times d^2 \times F_{uf}}\right]\right] \times F_{uf} \quad (4)$$

$$V_{rfn} = 0.62 \times F_{uf} \times 0.56 \times d^2 \quad (5)$$

Where, $\mu$ is the friction coefficient at the sliding interfaces between the slotted plate and the shims, $d$ is the bolt nominal diameter, $F_{uf}$ is the bolt nominal ultimate tensile strength, and $l$ is the bolt lever arm. In this model, the bolt axial tension during the sliding, $T$, can be obtained by solving the quadratic equation resulting from substituting Equations 2 to 5 into Equation 1, and defined:

$$-T^2 \times (3.0 \times \mu) + T \times (F_{uf} \times d) \times [(1.75 \times \mu \times l) + (1.65 \times \mu \times d) + 1.05] - (0.58 \times F_{uf}^2 \times d^4) = 0 \quad (6)$$

Recently, the effect of the bolt inclination have been introduced in previous MPV models (Chanchi et al. 2019b). This improved model is based on considering the bolt inclination angle. Here, this angle is termed elastic inclination angle, $\theta e$, since the bolt reaches this angle before flexural yielding occurs on the bolt shank. The elastic inclination angle is calculated:

$$\theta e = tan^{-1}\left[\frac{O}{tf}\right] \quad (7)$$

Where, $O$ is the bolt hole oversize, and $tf$ is the fixed plate thickness. Models described above seem to fit to the available AFCs experimental data for Bisalloy 400 and Bisalloy 500 shims (Khoo et al. 2014, Chanchi et al. 2019b). However, these models do not assess or do not consider:

1. The sliding strength at the first sliding of the slotted plate termed breakaway,
2. The effect of the horizontal component of the bolt tension, $Tsin\theta e$, shown in Figure 2c, and due to bolt inclination, on the sliding strength,
3. The effect of bolt behaviour across the development of the sliding strength on the hysteresis loop shape.

In order to quantify the above needs, AFC testing was undertaken, and a model was proposed by including the above variables on the Clifton 2005 and Khoo et al. 2014 MPV model. For that reasons this paper seeks answers to following questions:

1. What is the hysteresis loop shape during the development of the sliding strength?
2. What is the bolt behaviour during the development of the sliding strength?
3. Can a simple model be developed to assess the sliding strength considering the MPV effect and the horizontal component of the bolt tension due to the inclination effect?

## 2 MATERIALS AND METHODS

### 2.1 AFC devices and assembly

A total of 18 AFCs divided in 6 groups of 3AFCs were assembled. Each group of AFCs was assembled with slot length of 80mm, 2 M16 Grade 8.8 bolts, 6mm thick Bisalloy 500 shims, and Grade 300 steel for the cap, slotted, and fixed plates, as shown in Figures 2a –b. Bolts were supplied by Black Fasteners – New Zealand, and they were assembled with a structural washer below the bolt head and with a flat washer and a single Belleville washer below the nut, as shown in Figures 2a –b. Belleville washers were supplied by JamesGlen Stainless Fasteners – New Zealand, and they were used to keep the bolt assembly tension constant during testing (Khoo et al. 2014). Assembly dimensions for the 6 groups of AFCs are listed in Table 1.

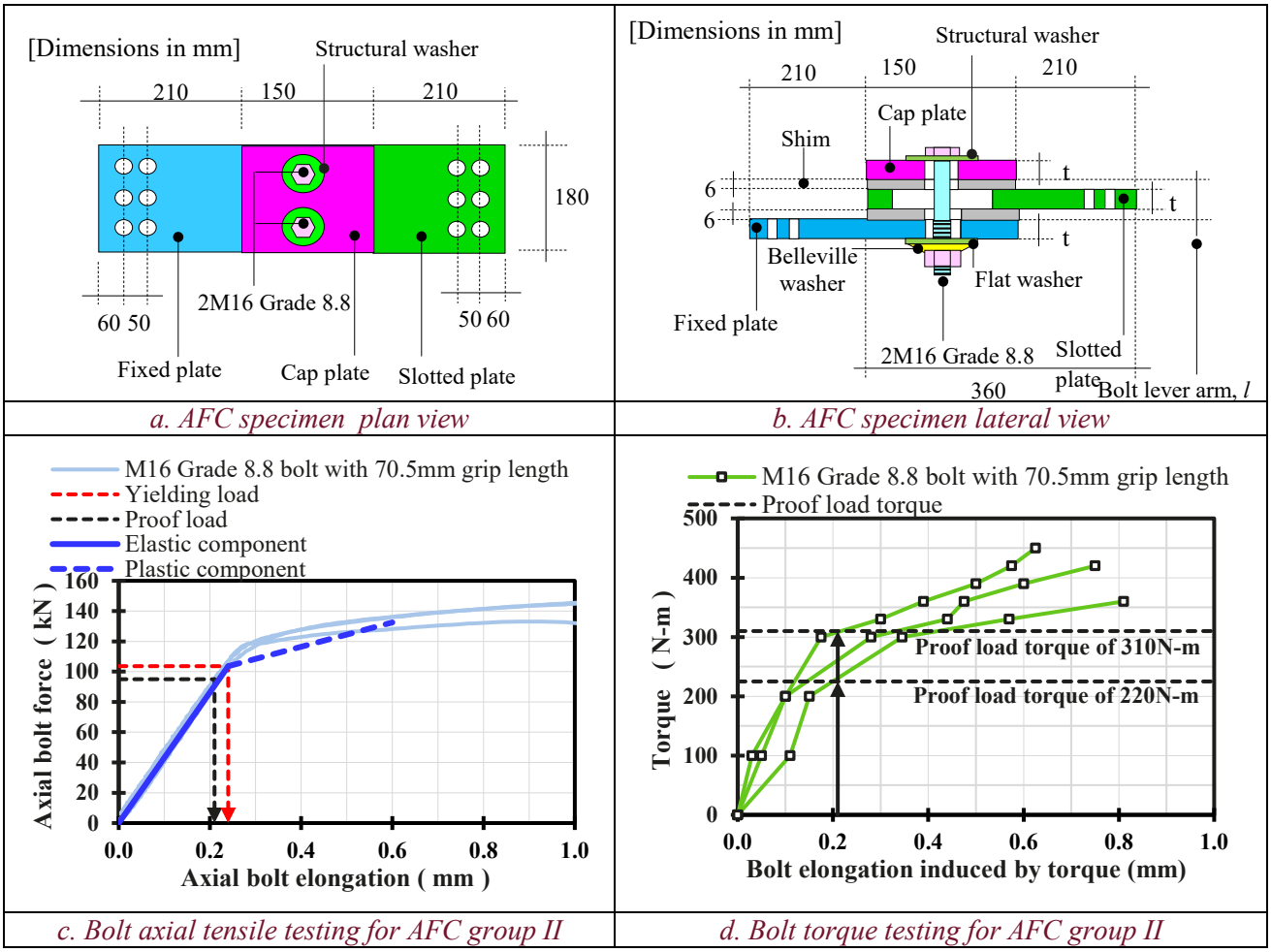


*a. AFC specimen plan view* | *b. AFC specimen lateral view*

*c. Bolt axial tensile testing for AFC group II* | *d. Bolt torque testing for AFC group II*

*Figure 2: AFC specimen and assembly relationships*

Prior to AFC assembly, the Bisalloy shims and the cap, fixed and slotted plates were cleaned with a rag and a thin layer of acetone for removing impurities from the bare surfaces. Each AFC was assembled using the torque control method. In this method, the M16 Grade 8.8 bolts were tensioned to the proof load of 95kN increasing gradually the torque up to the assembly torque value listed in Table 1. Here, the torque control method was used to systematically control the increase in bolt tension and bolt elongation using the experimental assembly relationships shown in Figures 2c – d. The assembly torque was defined as the torque that develops a bolt elongation termed proof load elongation defined as the elongation that a bolt develops in an axial tensile testing when it reaches the proof load. For each AFC group, the proof load elongation and the assembly torque listed in Table 1 were determined as the average of the values obtained from an axial tensile testing and a torque testing of 3 bolts with a testing length equal to the bolt grip length listed in Table 1. Figures 2c – d show the bolt axial tensile testing and the bolt torque testing for AFC group II. In the torque testing, a bolt was subjected to a torque increased gradually until the bolt elongation was equal to the proof load elongation. The bolt elongations were measured in the bolt axial tensile testing with an extensometer with an accuracy of ±0.0001mm, and in the bolt torque testing with a micrometre with an accuracy of ±0.01mm. Before assembling AFCs, installation of 2 bolts per AFC group was inspected by comparing the curve torque – induced elongation obtained during the installation of the 2 bolts with the assembly relationship defined in Figure 2d and described above.

*Table 1: Assembly dimensions and inclination effect for the 6 groups of AFCs*

| AFC Group | Grade 300 steel plates thickness $t$ mm | Bolt grip length outside of washers $G$ mm | Bolt size | Bolt shank unthreaded length mm | Bolt shank threaded length mm | Bolt lever arm $l$ mm | Ratio of bolt lever arm to bolt diameter $l/d$ mm/mm | Proof load elongation $\delta_{proof}$ mm | Proof load torque $T_{proof}$ N-m | Bolt elastic inclination angle $\theta e$ radians | Slotted plate displacement for bolt elastic inclination angle $\Delta e$ mm |
|---|---|---|---|---|---|---|---|---|---|---|---|
| I | 10 | 52.5 | M16 x 80 | 42.0 | 38.0 | 22.0 | 1.4 | 0.152 | 245 | 0.20 | 5.2 |
| II | 16 | 70.5 | M16 x 90 | 52.0 | 38.0 | 28.0 | 1.8 | 0.199 | 265 | 0.12 | 4.4 |
| III | 25 | 97.5 | M16 x 120 | 82.0 | 38.0 | 37.0 | 2.3 | 0.259 | 310 | 0.08 | 3.9 |
| IV | 30 | 112.5 | M16 x 140 | 96.0 | 44.0 | 42.0 | 2.6 | 0.295 | 315 | 0.07 | 3.7 |
| V | 40 | 142.5 | M16 x 180 | 136.0 | 44.0 | 52.0 | 3.2 | 0.357 | 335 | 0.05 | 3.6 |
| VI | 50 | 172.5 | M16 x 200 | 156.0 | 44.0 | 62.0 | 3.9 | 0.433 | 365 | 0.04 | 3.4 |

## 2.2 Quasi-static testing

AFCs were quasi-statically tested on horizontal test setup fitted in a shake table, as shown in Figure 3a. In this test setup, one of the AFC ends was bolted to a fixed bracket connected to a reaction tower and the other AFC end was bolted to a moving bracket connected to reaction frame on the shake table.

The test setup was instrumented with a load cell in series with the fixed bracket and with potentiometer placed across the AFC stroke, as shown in Figure 3. The sliding mechanism of the AFC was activated by a displacement regime comprising 18 sinusoidal cycles with amplitudes of 1.5mm – 20mm, as shown in Figure 3b. The maximum amplitude of the displacement regime of ± 20mm corresponds to 50% of the slot length of 80mm. The displacement regime was run twice with a break time of 30minutes between runs for removing the AFCs friction heat. No bolt re-tensioning was undertaken for the second run.

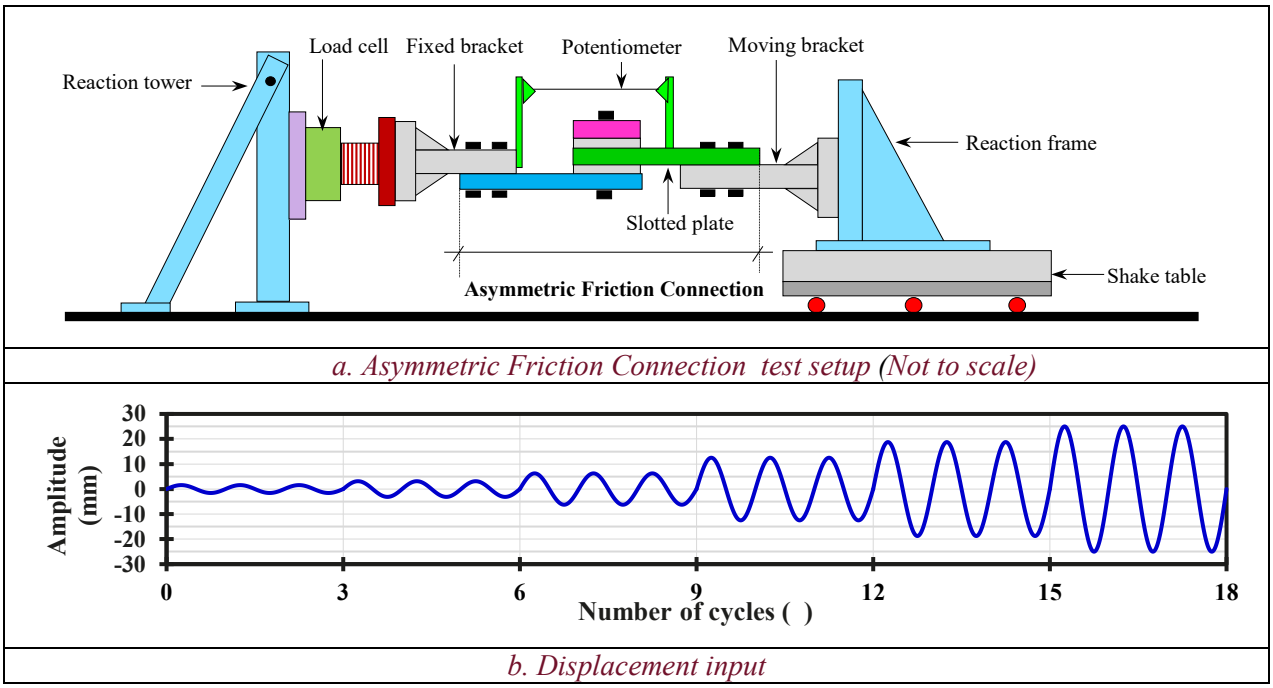


*a. Asymmetric Friction Connection test setup (Not to scale)*

*b. Displacement input*

*Figure 3: AFCs test setup and displacement input*

## 2.3 AFC scaled prototype

A prototype of the AFC lateral view shown in Figure 2b was assembled in scale of 30% of the full scale lateral view of the AFCs for group VI in Table 1. The AFC scaled prototype was assembled using plasticine for the bolt, and wood pieces for the Grade 300 steel plates and for the Bisalloy 500 shims, as shown in Figure 4a. In the AFC scaled prototype the bolt head, nut and washers are ignored, and bolt and plates are assembled ignoring the bolt clamping force, as shown in Figure 4b. In the AFC scaled prototype, the sliding mechanism of the AFCs can be reproduced by displacing the plates by hand, and the bolt performance during sliding is reproduced as the plates push the bolt.

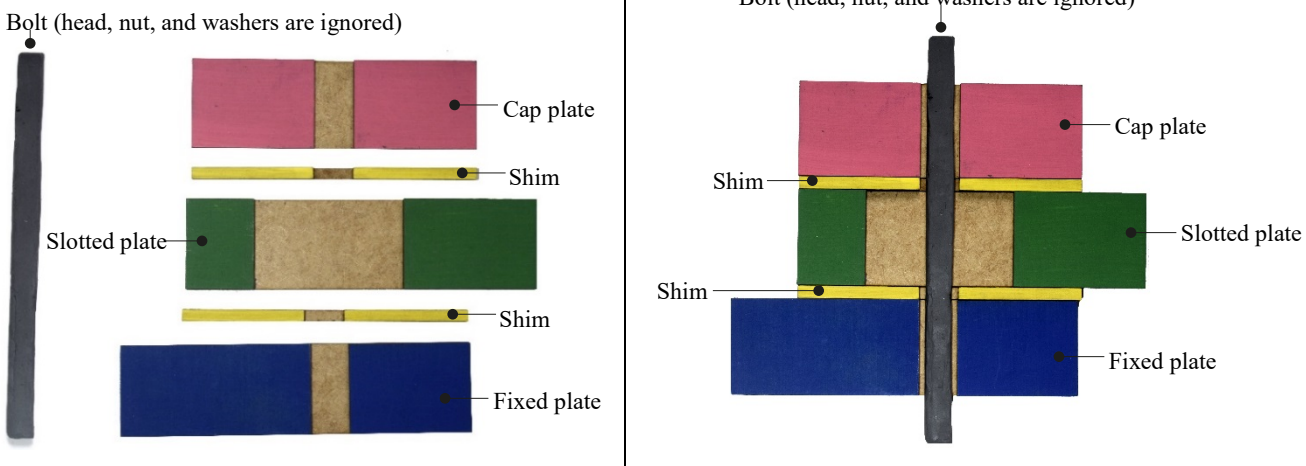


*a. AFC scaled prototype components*

*b. AFC scaled prototype assembly*

*Figure 4: AFC scaled prototype*

# 3 RESULTS AND ANALYSIS

## 3.1 Hysteresis loop shape with the displacement amplitude

Figure 5 shows the hysteresis loop for AFCs with ratios of the bolt lever arm to the bolt diameter, *l/d*, of 1.4 – 2.9. The hysteresis loop is shown before breakaway, and for displacement amplitudes of 3mm – 6mm, and 12mm – 20mm. The displacement amplitudes of 3mm – 6mm and 12mm – 20mm match with the displacement amplitudes equal and greater than to those the slotted plate slid for the elastic bolt inclination angle, $\theta e$, and calculated as the product of $\theta e$ and half of the bolt grip length outside of washers *G,* as

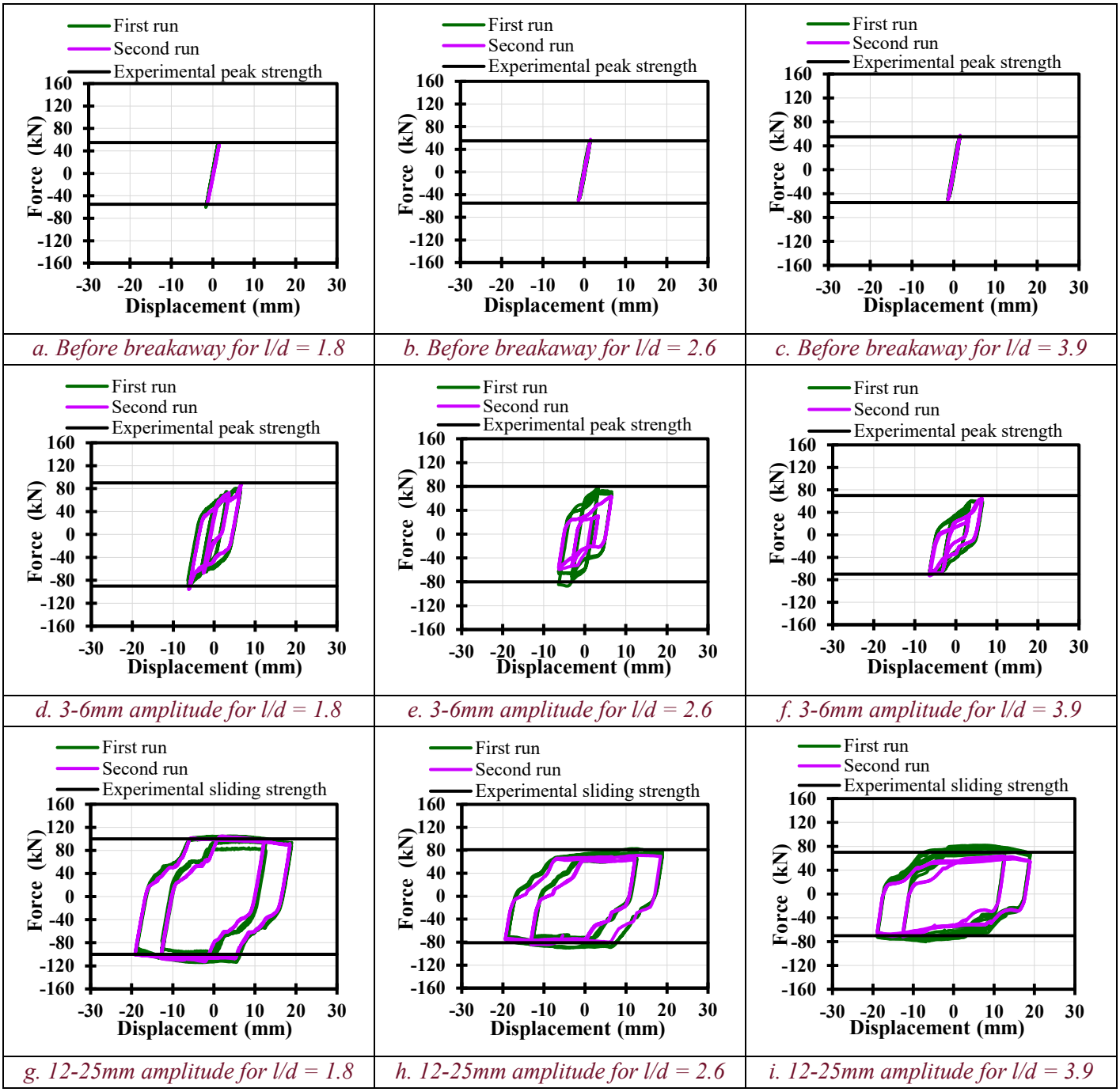


*a. Before breakaway for l/d = 1.8* | *b. Before breakaway for l/d = 2.6* | *c. Before breakaway for l/d = 3.9*

*d. 3-6mm amplitude for l/d = 1.8* | *e. 3-6mm amplitude for l/d = 2.6* | *f. 3-6mm amplitude for l/d = 3.9*

*g. 12-25mm amplitude for l/d = 1.8* | *h. 12-25mm amplitude for l/d = 2.6* | *i. 12-25mm amplitude for l/d = 3.9*

*Figure 5: Hysteresis loop for bolt lever arms l = 22mm – 62mm at displacement amplitudes 1.5mm – 20mm*

shown in Table 1. The hysteresis loop shape is linear before breakaway, bilinear for displacement amplitudes equal to those the slotted plate slid for $\theta e$, and rectangular and pinched for displacement amplitudes greater than those the slotted plate slid for $\theta e$. Figures 5a – c show regardless of the $l/d$, the peak force before breakaway was same. That is because the bolt is near to vertical with minor MPV or inclination effects, therefore the AFC strength depends only on the friction force induced by the bolt assembly force. Figures 5d – f show the peak force for the bilinear hysteresis loops reduced slightly as $l/d$ increased. That is because the bolt inclination was equal to $\theta e$, which indicates the AFC strength depends on the friction force induced by the bolt assembly force reduced by the MPV effect and increased slightly by the bolt inclination effect. The bolt inclination effect is not dominant, since the bolt inclination reduced with $l/d$, as shown in Table 1. Figures 5g – i show the average force across the flat zone of the rectangular and pinched hysteresis loop reduced as $l/d$ increased. That is because the AFC strength depends on the MPV and bolt inclination effects. The reduction in AFC strength due to MPV is exacerbated for lager displacements of the slotted plate since the cap plate is dragged against the bolt by the slotted plate, which increases the bolt inclination and produces bolt yielding; thus increasing the AFC strength reduction.

### 3.2 Bolt inclination with the displacement amplitude

Figure 6 shows the AFC scaled prototype and the bolt free body diagram, both during the development of the AFC strength. For the AFC At rest, the bolt was vertical, centred in the fixed plate bolt hole, and was under the assembly bolt tension, $A$, as shown in Figure 6a. Before breakaway, the bottom shim and the slotted plate slid pushing the bolt until the bolt inclined slightly while bearing on the fixed plate. The assembly bolt tension, $A$, increased slightly due to a force termed inclination force, $I$, resulting from the equilibrium of the moment produced by the friction force developed at the bottom shim – fixed plate interface $0.5P$ and the bolt lever arm, $l$, as shown in Figure 6b. These results indicate before breakaway the bolt is under the MPV and inclination effects. However, both effects are not significant since the bolt lever arm $l$ and the breakaway inclination angle $\theta b$ are well below than those the bolt develops for the elastic inclination angle $\theta e$

As the force F pushing the slotted plate increased, sliding of the top shim and the cap plate are activated, and the bolt is pushed and forced to incline in the opposite direction until reaching the elastic inclination angle θe. Since the bolt lever arm l, and the moment on the bolt increased respect to those before breakaway, as shown in Figures 6b - c, the combined action of MPV and the inclination effect for the elastic bolt inclination θe are greater than those before breakaway. As a result of the MPV effect, the bolt assembly tension is reduced to a bolt tension N*, and the inclination force I increased, and as a result of the bolt inclination effect, the horizontal components of the bolt tension, Tsinθe increased. It should be noted when the bolt reached θe, the bolt was bearing not only on the cap plate – top shim and fixed plate – bottom shim interfaces, but also on the cap and fixed plates, which generated the horizontal bearing force B, as shown in Figure 6c. Actual design practice does not consider both, the bolt tension horizontal component Tsin θe or the bearing force B.

If after the bolt reaches θe, the bolt demand from MPV effect is big enough to yield the bolt in bending, two plastic hinges will appear on the bolt shank at the location of the cap plate – top shim interface and at the location of the fixed plate – bottom shim interface, as shown in Figure 6d. These plastic hinges increase the bolt inclination from θe to an inclination angle termed yielding inclination angle, θy, as shown in Figure 6d. As a result of the increase in inclination angle, the horizontal component of the bolt tension increased to Tsin θy producing an increase in the AFC strength. However, the inclination force I remains constant since the bolt yielded. These results indicate the maximum effect of the horizontal component of the bolt tension on the AFC strength occurred after the bolt yield in bending. It should be noted, to date, the yielding inclination angle θy, has not been considered in design.

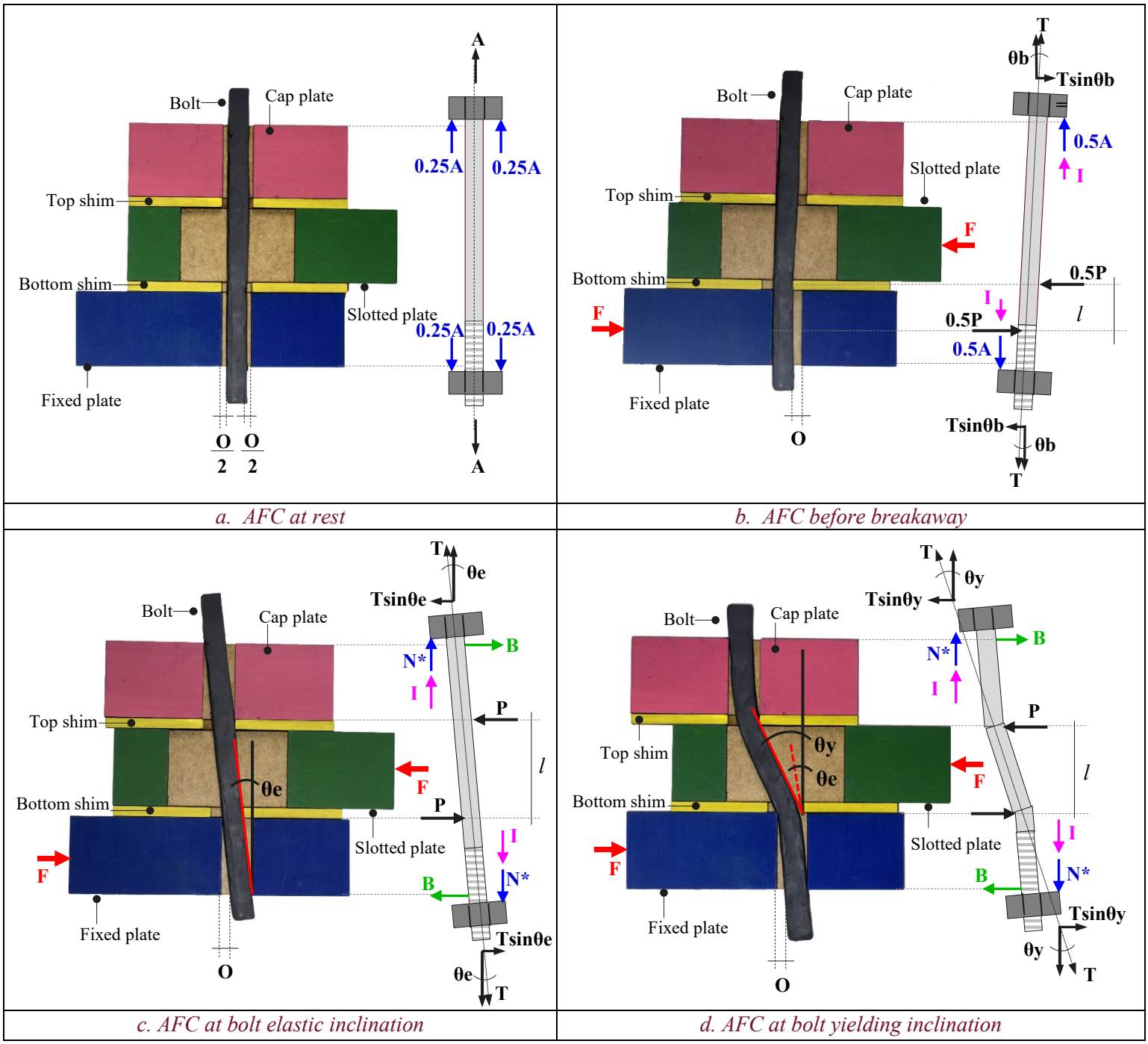


a. AFC at rest

b. AFC before breakaway

c. AFC at bolt elastic inclination

d. AFC at bolt yielding inclination

*Figure 6: Observed bolt behaviour on the AFC scaled prototype and idealized bolt free body diagram*

## 4 PROPOSED AFC STRENGTH MODEL AND HYSTERESIS LOOP SHAPE

Before breakaway, the hysteresis loop shape is proposed to be linear, as shown in Figure 7a. The peak strength is represented by the force required to overcome the friction induced by the assembly bolt tension at the bottom shim – slotted plate interface. No MPV or inclination effects are considered since the bolt is near vertical. The peak strength before breakaway, Pb, is calculated:

| | |
|---|---|
| $Pb = m \times \mu \times F_{proof}$ | (8) |

Where, m is the number of bolts, $\mu$ is the friction coefficient at the sliding interfaces, and $F_{proof}$ is the proof load per bolt.

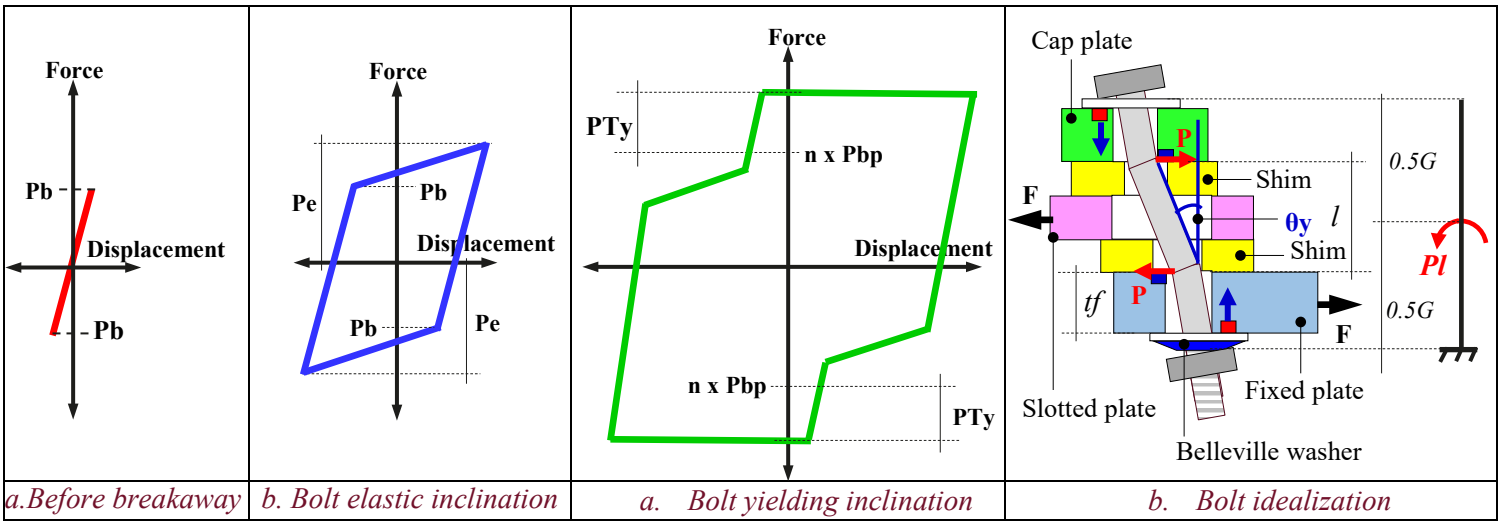


*a.Before breakaway* | *b. Bolt elastic inclination* | *a. Bolt yielding inclination* | *b. Bolt idealization*

*Figure 7: Variation of the idealized hysteresis loop with the displacement amplitude*

For displacement amplitudes producing the bolt elastic inclination, the hysteresis loop shape is proposed to be bilinear, as shown in Figure 7b. The strength is represented by the peak strength before breakaway plus the force required to overcome the friction induced by the sliding bolt tension in the top shim – fixed plate interface, and plus the horizontal component of the bolt sliding tension produced when the bolt inclines the elastic inclination angle. The bolt sliding tension, is the bolt tension force including the reduction in strength due to MPV, and it is considered only for the top shim – fixed plate interface and the inclination effect since the reduction due to MPV occur after the breakaway and when bolts reach the elastic inclination angle. The peak strength at the bolt elastic inclination, *Pe*, is calculated:

$$Pe = Pb + (m \times \mu \times T) + (m \times T \times sin\theta e) \quad (9)$$

Where, *Pb* is the peak strength before breakaway defined by Equation 8, *m* is the number of bolts, $\mu$ is the friction coefficient at the sliding interfaces, *T* is the bolt sliding tension obtained by solving Equation 6, and $\theta e$ is the bolt elastic inclination angle defined by Equation 7. The third component of Equation 9 is *PTe* and corresponds to the horizontal component of the bolt sliding tension produced when bolts reach $\theta e$.

For displacement amplitudes producing the bolt yielding inclination, the hysteresis loop shape is proposed to be square and pinched, as shown in Figure 7c. The average strength across the flat zone of the hysteresis loop (sliding strength) is represented by the force that activates the sliding at the bottom shim – fixed plate and top shim cap plate interfaces plus the horizontal component of the bolt sliding tension produced when bolts reach the yielding inclination angle. These two components are function of the bolt sliding tension since for the bolt yielding inclination, bolts have been through the MPV effect. The sliding strength at the bolt yielding inclination, *Py*, is calculated:

$$Py = (n \times m \times \mu \times T) + (m \times T \times (sin\theta e + sin\theta y)) \quad (10)$$

$$Py = (n \times Pbp) + PTy \quad (11)$$

Where, *n* is the number of sliding interfaces, *m* is the number of bolts, $\mu$ is the friction coefficient at the sliding interfaces, *T* is the bolt sliding tension obtained by solving Equation 6, and $\theta y$ is the bolt yielding inclination angle. Equation 10 can be also expressed in terms of the force required to activate each sliding

interface, *Pbp*, and the horizontal component of the bolt sliding tension produced when bolts reach the yielding inclination angle, *PTy*, as shown in Equation 11 and Figure 7c. The bolt yielding inclination angle $\theta y$ in Equation 10 can be calculated by idealizing the bolt as cantilever beam under a concentrated moment on half of the bolt grip length, and with a built in support at the interface between the nut and the Belleville washer, as show in Figure 7d. In this idealized bolt model, $\theta y$ is calculated as the ratio between the bolt head horizontal displacement considering the bolt plastic modulus, and the bolt grip length minus the fixed plate thickness, as shown in Equation 12. The bolt plastic modulus is considered since bolts yield either axially due to the increase in bolt tension from bolt inclination, or in bending due to MPV.

$$\theta y = \frac{3 \times \mu \times T \times l \times G^2}{8 \times Ep \times I \times (G - tf)} \quad (12)$$

Where, $\mu$ is the friction coefficient at the sliding interfaces, $T$ is the sliding tension obtained by solving Equation 6, $l$ is the bolt lever arm, $G$ is the bolt grip length outside of washers, $Ep$ is the bolt plastic modulus, $I$ is the bolt inertia for the bolt nominal diameter, and $tf$ is the fixed plate thickness.

The proposed model described above ignores the reduction in strength due to degradation of the sliding surfaces, which include loss of bolt tension and reduction in friction coefficient at the sliding surfaces. This reduction in strength is not considered since assessment is complex, and there is not model ready available.

## 5 COMPARISON BETWEEN MODEL AND EXPERIMENTAL RESULTS

Figure 8 compares the experimental AFC strength with the AFC strength predicted with the proposed model described in Section 4 and based on Equations 1 – 12. This comparison was undertaken for AFCs with ratios of bolt lever arm to bolt diameter, *l/d*, of 1.4 – 2.9, and before breakaway, and for displacement amplitudes of 3mm – 6mm, and 12mm – 20mm. These displacement amplitudes match with those producing the elastic bolt inclination and the yielding bolt inclination, respectively.

Values of the experimental AFC strength are represented in Figure 8 by the black solid line, and were red from the hysteresis loops. Values of the predicted AFC strength are represented in the Figure 8 by the red dotted line and were obtained from Table 2. In Table 2, the predicted AFC strength was calculated for a friction coefficient at the sliding interfaces $\mu = 0.22$, a bolt proof load $Fproof = 95kN$, two bolts $m = 2$, two sliding interfaces $n = 2$, a bolt nominal diameter $d = 16mm$, a bolt inertia for the bolt nominal diameter $I = 3217mm^4$, a bolt hole oversize $O = 2mm$, and a bolt plastic modulus $Ep = 3600MPa$. The plastic modulus was obtained from the plastic component of the bilinear – model fitted on the bolt axial tensile testing relationship shown in Figure 2c. The plastic modulus was obtained as the ratio between a bolt axial plastic stress of *184.08MPa* calculated for the bolt tension area of $157mm^2$ and a bolt axial plastic strain of *0.00511mm/mm* calculated for the bolt testing length of *70.5mm*, which corresponds to the bolt grip length of the AFC group II in Table 1. The bolt sliding tension $T$ in Table 2 was obtained by solving Equation 6 considering the parameters listed above, a bolt tensile ultimate strength $Fuf = 830MPa$, and the bolt lever arms indicated in Table 2. For the 6 groups of AFCs in Table 2, the bolt lever arm $l$ and the bolt grip length outside of washers $G$ were taken from Table1.

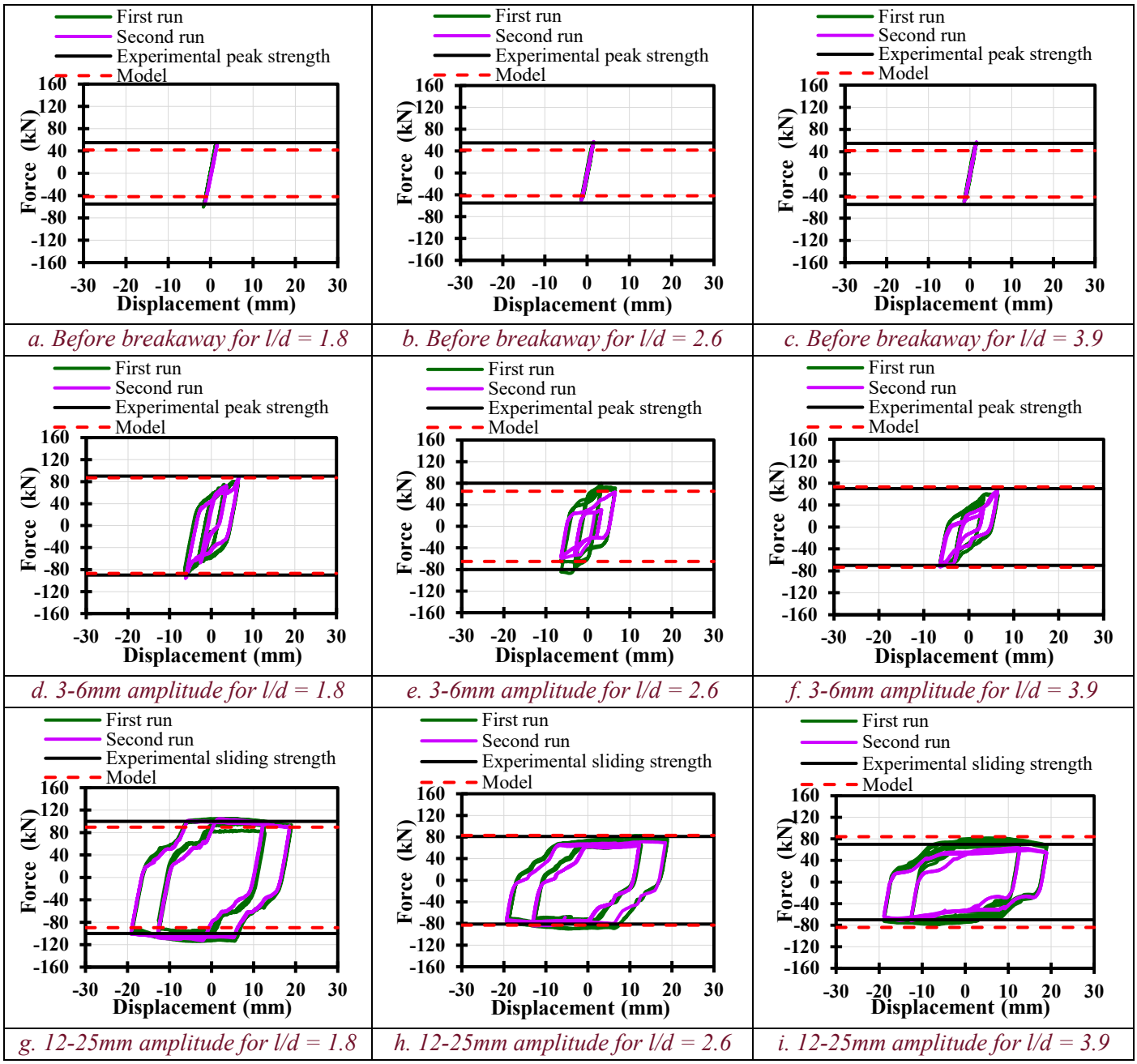


*Figure 8: Comparison of the sliding strength model with the experimental results for AFCs with l/d = 1.4 - 2.9*

Figure 8 shows the predicted AFC strength agrees well with the experimental values. Table 2 indicates the proposed model predicts the experimental AFC strength with accuracies of 76% – 120% before breakaway, and for bolt elastic and yielding inclination angles. These results indicate the proposed model predicts the AFC strength with good accuracy. Discrepancies between the experimental and predicted values are attributed to variability of the bolt assembly force, and reductions in friction coefficient at the sliding interfaces due to surface degradation, which were not considered in the proposed model. Table 2 shows the contribution in AFC strength of the horizontal component of the bolt tension from the bolt inclination effect was 6% - 28% for the bolt elastic inclination, and 38% - 53% for the bolt yielding inclination.

*Table 2: Experimental and predicted strength for AFCs with l/d l/d = 1.4 - 2.9*

| AFC group | Bolt inclination angle | | Bolt sliding tension | Peak strength before breakaway | | | Peak strength at the bolt elastic inclination | | | | | Average sliding strength at the bolt yielding inclination | | | | |
|---|---|---|---|---|---|---|---|---|---|---|---|---|---|---|---|---|
| | Elastic | Yielding | | Measured | Model | Accuracy | Measured | Model | Accuracy | Inclination effect | | Measured | Model | Accuracy | Inclination effect | |
| | *θe* Degrees | *θy* Degrees | *T* kN | *Pb* kN | *Pb* kN | *A* % | *Pe* kN | *Pe* kN | *A* % | *PTe* kN | *PTe/Pe* % | *Py* kN | *Py* kN | *A* % | *PTy* kN | *PTy/Pp* % |
| I | 11.3 | 4.2 | 71.9 | 50 | 42 | 84 | 93 | 102 | 110 | 28.2 | 28 | 105 | 102 | 97 | 38.7 | 38 |
| II | 7.1 | 6.8 | 65.6 | 55 | 42 | 76 | 90 | 87 | 97 | 16.3 | 19 | 99 | 90 | 91 | 31.9 | 35 |
| III | 4.6 | 11.5 | 58.3 | 55 | 42 | 76 | 78 | 77 | 99 | 9.3 | 12 | 90 | 84 | 93 | 32.6 | 39 |
| IV | 3.8 | 14.4 | 54.9 | 55 | 42 | 76 | 63 | 73 | 116 | 7.3 | 10 | 88 | 83 | 94 | 34.7 | 42 |
| V | 2.9 | 20.7 | 49.2 | 53 | 42 | 79 | 90 | 68 | 76 | 4.9 | 7 | 85 | 83 | 98 | 39.7 | 48 |
| VI | 2.3 | 27.5 | 44.7 | 55 | 42 | 76 | 80 | 65 | 81 | 3.6 | 6 | 70 | 84 | 120 | 44.9 | 53 |

## 6 CONCLUSIONS

This paper describes the effect of the displacement amplitude on the hysteresis loop shape, on the bolt behaviour during sliding, and on the strength of AFCs with ratios of the bolt lever arm to bolt diameter *l/d* of 1.4 – 3.9. It is shown that:

1. The hysteresis loop shape of AFCs is linear before breakaway, bilinear for the bolt elastic inclination, and square and pinched for the bolt yielding inclination. Before breakaway, regardless of *l/d* value, the peak strength is constant since the bolt is near vertical and the MPV and inclination effects are minor. For the elastic and yielding bolt inclination angles, the peak strength and the sliding strength, respectively, reduced as *l/d* increased due to reductions in strength from MPV effect and the reductions in the elastic inclination angle.
2. The bolt inclination increases with the displacement amplitude from near vertical to the yielding inclination angle. Before breakaway, bolts are vertical and the bolt tension remains near to the assembly force, since the MPV and the inclination effects are minor. For the bolt elastic inclination angle, the bolt tension increases due to significant MPV effect. The maximum inclination effect occurs when bolts reach the yielding angle after bolts yield due to MPV, which produces plastic hinges on the bolt shanks, thus increasing significantly the bolts inclination. In the current AFCs design practice, the horizontal component of the bolt sliding tension from the inclination effect, as well as the yielding inclination angle are not considered.
3. A simple model to assess the strength of AFCs considering the friction component influenced by the bolt MPV effect, and the horizontal component of the bolt tension from the bolt inclination effect was proposed. The proposed model can be used for predicting the peak strength before breakaway and for the elastic bolt inclination, and for predicting the sliding strength for the yielding bolt inclination. The model agrees well with the experimental data and predicts the AFC strength with accuracies of 76% – 116%. The proposed model shows the horizontal component of the bolt tension from the bolt inclination effect was 6% - 28% of the AFC strength for the bolt elastic inclination, and 38% - 53% of the AFC strength for the bolt yielding inclination.

## REFERENCES


Clifton, G.C. 2005. Semi-Rigid Joints for Moments Resisting Steel Framed Seismic Resisting Systems. *Published PhD Thesis, Department of Civil and Environmental Engineering.* University of Auckland – New Zealand.

Bisalloy Steels Pty Ltd. 2006. Bisalloy Technical Manual. *Bisalloy Steels Pty Ltd.* Unanderra – Australia.

Rodgers, G.W., Chase, J.G., Causse, R., Chanchi Golondrino, J.C. and MacRae, G.A. 2017. Performance and Degradation of Sliding Steel Friction Connections: Impact of Velocity, Corrosion Coating and Shim Material. *Engineering Structures,* Vol. 141, pp. 292–302. ISSN: 0141-0296.

MacRae, G.A., Clifton, C.G., MacKinven, H., Mago, N., Butterworth, J., Pampanin, S. 2010. The Sliding Hinge Joint Moment Connection. *Bulletin of the New Zealand Society for Earthquake Engineering,* Vol. 43, Issue 3, p. 202-212.

Xie, R., Chanchi, J.C., MacRae, G.A., and Clifton, C.G. 2018. Braced frame asymmetrical and asymmetrical friction connection performance. *Key Engineering Materials,* Vol. 763, pp. 216 – 223.

Borzouie, J., Chase, J.G., MacRae, G.A. and Rodgers, G.W. 2015. Experimental Studies on Cyclic Performance of Column Base Weak Axis Aligned Asymmetric Friction Connection. *Journal of Constructional and Steel Research (JCSR),* Vol. 112, pp. 252-262

Chanchí Golondrino, J. C., MacRae, G. A., Chase, J. G., Rodgers, G. W., Clifton, G. C. 2019a. Asymmetric Friction Connection (AFC) Design for Seismic Energy Dissipation. *Journal of Constructional Steel Research,* Vol. 157, pp. 70-81.

Khoo, H.H., Clifton, G.C., MacRae, G.A., Zhou, H., and Ramhormozian, S. 2014. Proposed design models for the asymmetric friction connection. *Earthquake and Structural Dynamics Journal,* Vol. 44, Issue 8, p. 1309-1324.

Chanchí Golondrino, J.C. 2019b. Hysteretic behaviour of Asymmetric Friction Connections (AFCs). *Unpublished PhD Thesis, Department of Natural and Civil Engineering Resources.* University of Canterbury - New Zealand.